Ti_5Si_3 Nanowire and Its Field Emission Property

Huang-Kai Lin,[†] Yu-Fen Tzeng,[‡] Chia-Hsin Wang,[†] Nyan-Hwa Tai,[‡] I-Nan Lin,[§] Chi-Young Lee,*[,‡] and Hsin-Tien Chiu*[,†]

Department of Applied Chemistry, National Chiao Tung University, Hsinchu, Taiwan 30050, R.O.C., Department of Materials Science and Engineering and Center for Nanotechnology, Materials Science, and Microsystems, National Tsing Hua University, Hsinchu, Taiwan 30043, R.O.C., and Department of Physics, Tamkang University, Taipei, Taiwan 25137, R.O.C.

Received October 2, 2007
Revised Manuscript Received February 22, 2008

Because of their distinct properties, one-dimensional (1D) nanostrutures have attracted a tremendous amount of attention for technological applications, such as sensors,[1] laser devices,[2] and electrical systems.[3] An increasing effort has been devoted to fabricating nanomaterials for new field emitters, such as CNTs (carbon nanotubes),[4] nanodiamond coated Si nanowires (NWs), [5] SiC NWs and nanotubes,[6] metal oxides,[7] and metal silicides.[8] Many studies about the fabrication of free-standing silicide NWs of Ti, Cr, Fe, Co, Ni and Ta have been reported because of their superior properties and compatibility with Si based integrated circuit devices.[8–14] Among them, titanium silicides are potential candidates for field emission devices due to their relative low resistivity (10–28 $\mu\Omega$ cm), high thermal stability, and low work function.[15–17] Research on the fabrication of TiSi and $TiSi_2$ NWs and arrays through various processing techniques, including chemical vapor deposition (CVD) and physical vapor deposition (PVD), have been demonstrated recently.[9,18–20] On the other hand, fabrication of nanostructures of metal-rich titanium silicide Ti_5Si_3, which is a suitable refractory material with a melting point 2403 K, has not been reported. In this work, we report the first growth of Ti_5Si_3 NWs via a unique CVD process.[21] Microstructures and field emission properties of the NWs will be discussed in detail.

Table 1. Summary of Samples

sample	growth conditions	morphologies and phases	E_0[a] (V/μm)	β[b]
I	973 K,6h	Ti_5Si_3 NWs/C54-$TiSi_2$ film	5.4	816
II	773 K,6h	*a*-Ti_xSi_y NWs/C54-$TiSi_2$ film	7.6	*c*
III	973K,1h	C54-$TiSi_2$ film	10.4	343

[a] Turn-on field. [b] Field enhancement factor. [c] Cannot be obtained due to the lack of work function of amorphous Ti_xSi_y.

All reactions were performed in a low pressure horizontal hot-wall quartz tube reactor heated by a three-zone tube furnace. $TiCl_4$, the precursor, was vaporized into the reaction chamber at a controlled partial pressure. Close to the precursor inlet, Ti powders were placed at the heating zone at 1173 K. Si(100) wafers were placed at the center heating zone at 773–973 K. After 1–6 h, deposition of a gray layer on the substrates was observed. A summary of the representative samples prepared in this study is listed in Table 1. Figure 1 shows the morphology and the chemical composition of sample **I** grown at 973 K on Si for 6 h. Figure 1a is a top-view scanning electron microscopic (SEM) image of **I**. It displays that on top of a deposited thin film, there are a considerable amount of thread-like NWs a few micrometers long. A representative high-magnification SEM image in Figure 1b shows that the 1D nanostructures have diameters 20–50 nm. In addition, the image does not show evidence for the presence of metal particles, which may act as catalysts, on the tips of the wires. An energy-dispersive X-ray (EDX) spectrum of **I** in Figure 1c indicates that the sample contains Ti and Si only. A side view SEM image in Figure 1d reveals that numerous NWs of a few micrometers in length extend randomly from the top of a deposited film with a thickness of approximately 6 μm on Si. X-ray diffraction

* Corresponding authors. E-mail: cylee@mx.nthu.edu.tw (C.-Y.L.), htchiu@faculty.nctu.edu.tw (H.-T.C.).
[†] National Chiao Tung University.
[‡] Nationa Tsing Hua University.
[§] Tamkang University

(1) Cui, Y.; Wei, Q.; Park, H.; Lieber, C. M. *Science* **2003**, *293*, 1289.
(2) Huang, M. H.; Mao, S.; Yan, H.; Wu, Y.-Y.; Kind, H.; Weber, E.; Russo, R.; Yang, P.-D. *Science* **2001**, *292*, 1897.
(3) Huang, Y.; Duan, X.; Wei, Q.; Lieber, C. M. *Science* **2001**, *291*, 630.
(4) Heer, W. A.; Chatelain, A.; Ugarte, D. *Science* **1995**, *270*, 1179.
(5) Tzeng, Y.-F.; Lee, Y.-C.; Lee, C.-Y.; Lin, I-N.; Chiu, H.-T. *Appl. Phys. Lett.* **2007**, *91*, 063117.
(6) (a) Zhou, X.-T.; Lai, H.-.; Peng, H.-Y.; Au, F. C.-K.; Liao, L.-S.; Wang, N.; Bello, I.; Lee, C.-S.; Lee, S.-T. *Chem. Phys. Lett.* **2000**, *318*, 58. (b) Wang, C.-H.; Lin, H.-K.; Ke, T.-Y.; Palathinkal, T. J.; Tai, N.-H.; Lin, I-N.; Lee, C.-Y.; Chiu, H.-T. *Chem. Mater.* **2007**, *19*, 3956.
(7) Tseng, Y.-K.; Huang, C.-J.; Cheng, H.-M.; Lin, I-N.; Liu, K.-S.; Chen, I-C. *Adv. Funct. Mater.* **2003**, *13*, 811.
(8) Chueh, Y.-L.; Ko, M.-T.; Chou, L.-J.; Chen, L.-J.; Wu, C.-S.; Chen, C.-D. *Nano Lett.* **2006**, *6*, 1637.
(9) (a) Xiang, B.; Wang, Q.-X.; Wang, Z.; Zhang, X.-Z.; Liu, L.-Q.; Xu, J.; Yu, D.-P. *Appl. Phys. Lett.* **2005**, *86*, 243103. (b) Du, J.; Du, P. -Y.; Hao, P.; Huang, Y.-F.; Ren; Z.-D.; Han, G.-R.; Weng, W.-J.; Zhao, G.-L. *J. Phys. Chem. C* **2007**, *111*, 10814.
(10) (a) Seo, K.; Varadwaj, K. S. K.; Cha, D.; In, J.; Kim, J; Park, J.; Kim, B. *J. Phys. Chem. C* **2007**, *111*, 9072. (b) Szczech, J. R.; Schmmitt, A. L.; Bierman, M. J.; Jin, S. *Chem. Mater.* **2007**, *19*, 3238.
(11) (a) Quyang, L.; Thrall, E. S.; Deshmukh, M. M.; Park, H. *Adv. Mater.* **2006**, *18*, 1437. (b) Schmitt, A. L.; Bierman, M. J.; Schmeisser, Dieter.; Himpsel, F. J.; Jin, S. *Nano Lett.* **2006**, *6*, 1617. (c) Varadwaj, K. S. K.; Seo, K.; In, J.; Mohanty, P.; Park, J.; Kim, B. *J. Am. Chem. Soc.* **2007**, *129*, 8594.
(12) (a) Schmitt, A. L.; Zhu, L.; Schmeiber, D.; Himpsel, F. J.; Jin, S. *J. Phys. Chem. B* **2006**, *110*, 18142. (b) Seo, K.; Varadwaj, K. S. K.; Mohanty, P.; Lee, S.; Jo, Y.; Jung, M.-H.; Kim, J.; Kim, B. *Nano Lett.* **2007**, *7*, 1240.
(13) (a) Song, Y.; Jin, S. *Appl. Phys. Lett.* **2007**, *90*, 173122. (b) Song, Y.; Schmitt, A. L.; Jin, S. *Nano Lett.* **2007**, *7*, 965.
(14) Chen, L.-J. *Silicide Technology for Integrated Circuits*; IEE: London, 2004.
(15) Bucher, E.; Schultz, S.; Lux-Steiner, M. C.; Munz, P.; Gubler, U.; Greuter, F. *Appl. Phys. A: Mater. Sci. Process.* **1986**, *40*, 71.
(16) Maex, K.; Rossum, M. V. *Properties of Metal Silicides*; IEE: London, 1995.
(17) Murarka, S. P.; Fraser, D. B. *J. Appl. Phys.* **1980**, *51*, 350.
(18) Bennett, P. A.; Ashcroft, B.; He, Z.; Tromp, R. M. *J. Vac. Sci. Technol. B* **2002**, *20*, 2500.
(19) Hsu, H.-C.; Wu, W.-W.; Hsu, H.-F.; Chen, L.-J. *Nano Lett.* **2007**, *7*, 885.
(20) Choi, S.-S.; Jung, M.-Y.; Joo, M.-S.; Kim, D.-W.; Park, M.-J.; Kim, S.-B.; Jeon, H.- T. *Surf. Interface Anal.* **2004**, *36*, 435.
(21) Lee, C.-Y. *Chem. Vap. Deposition* **1999**, *5*, 69.

10.1021/cm800079c CCC: $40.75
Published on Web 03/11/2008

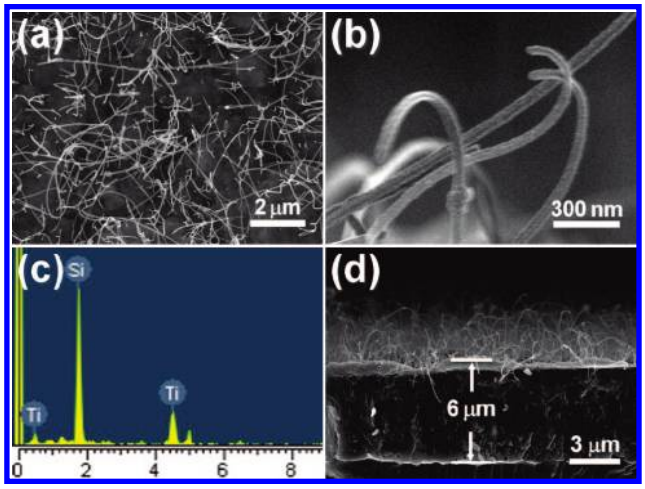

Figure 1. SEM images of sample **I** grown on Si. (a) Top view, (b) high magnification image, (c) EDX, and (d) side view image.

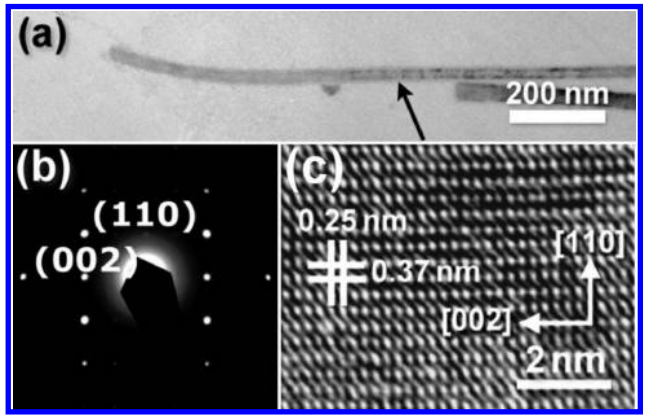

Figure 2. TEM studies of a NW isolated from **I**. (a) Low magnification image, (b) SAED pattern of the sample in part a showing a [1$\bar{1}$0] zone axis, and (c) high-resolution image from the selected section in part a.

(XRD) of **I** suggested that the film was composed mainly of orthorhombic C54-$TiSi_2$ phase (JCPDS 35-0785). However, transmission electron microscopic (TEM) studies of the NWs showed that the 1D material had a different titanium silicide phase. The presence of Ti metal powders at the heating zone at 1173 K was important for the successful NW growth. Without it, a $TiSi_2$ film with uneven surface was deposited on the Si substrate.

A typical TEM image of NWs isolated from **I** is shown in Figure 2a. It reveals a long NW with a diameter of approximately 30 nm. The image also confirms that on the tip of the wire, there is no evidence for the existence of any metal particles. A selected-area electron diffraction (SAED) image in Figure 2b, taken from the point indicated in Figure 2a, displays a dot pattern. This could be assigned to (002) and (110) planes of single crystalline hexagonal Ti_5Si_3 with a [1$\bar{1}$0] zone axis. Figure 2c is the high-resolution TEM (HRTEM) image taken at the same place. From the image, two sets of fringes spaced at 0.25 and 0.37 nm apart could be assigned to the lattice spacing of (002) and (110) planes of the Ti_5Si_3 phase, respectively. The wire growth direction is determined to be along the [002] axis of Ti_5Si_3. Thus, sample **I** is designated as Ti_5Si_3 NWs/$TiSi_2$. An Auger depth profile of **I** also confirmed that the sample contained a high

Scheme 1. Proposed Growth Steps of Ti_5Si_3 NWs

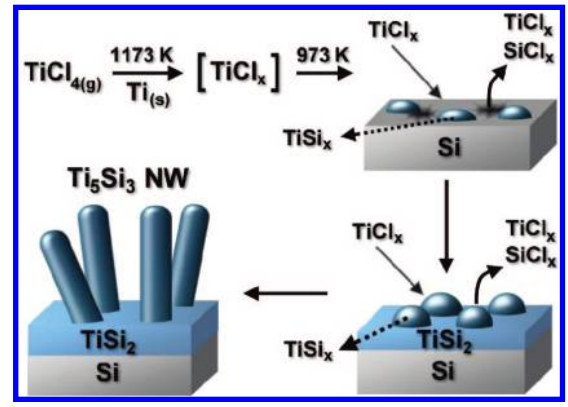

quantity of Ti on the surface while the Si content was rich inside the deposited layer.

Both reaction temperature and time were essential factors in the synthesis of the single crystalline Ti_5Si_3 NWs. When the reaction temperature was decreased to 773 K, sample **II** containing abundant amorphous Ti_xSi_y NWs on a C54-$TiSi_2$ thin film (designated as *a*-Ti_xSi_y NWs/$TiSi_2$) was produced in 6 h. As the reaction time was reduced to 1 h, sample **III**, which showed sparse and short NWs on a layer of C54-$TiSi_2$ thin film, was obtained. Consequently, we conclude that the titanium silicide 1D nanostructures could be fabricated only with sufficient reaction time. Furthermore, the crystal structures of the NWs depend highly on the reaction temperature.

Vapor–liquid–solid (VLS) growth is employed most frequently to account for the growth of many NWs. However, according to the observations discussed above, the VLS model can be ruled out easily, owing to the absence of metal particles on the tip of the NWs.[22] On the basis of the experimental observations, a plausible reaction pathway is proposed in Scheme 1 to rationalize the Ti_5Si_3 NW growth. It suggests that titanium subchlorides $TiCl_x$ ($x = 2, 3$), generated by the reaction between $TiCl_4$(g) and Ti metal in the high temperature zone at 1173 K initially, could serve as the Ti source in two ways.[23] One is their disproportionation into $TiCl_4$ molecules and Ti atoms in the low temperature zones below 973 K. The deposited Ti atoms could react with the Si surface atoms to form $TiSi_x$ clusters for further nucleation and growth. The second one is that $TiCl_x$ could react directly with the Si substrate to form Si-rich $TiSi_x$ clusters and gaseous $SiCl_x$ byproducts, which might serve as another Si source in the formation of $TiSi_x$.[24] As the reaction proceeds further, a $TiSi_2$ thin film is grown on the substrate. In the mean time, the disproportionation of the incoming $TiCl_x$ to deposit Ti atoms remains. But the supply of Si atoms either from the substrate or from the $SiCl_x$ byproducts could be hampered by the relative inertness of the as-formed $TiSi_2$ layer. In addition, the diffusion length of Si atoms from the substrate through the $TiSi_2$ layer

(22) Wagner, R. S.; Ellis, W. C. *Appl. Phys. Lett.* **1964**, *4*, 89.
(23) Ameen, M. S.; Leusink, G.; Hillman, J. T. U.S. Patent No. 5926737, 1999.
(24) (a) Reynolds, G. J.; Cooper, C. B.; Faczl, P. J. *J. Appl. Phys.* **1989**, *65*, 3212. (b) Southwell, R. P.; Seebauer, E. G. *J. Vac. Sci. Technol. A* **1995**, *13*, 221.

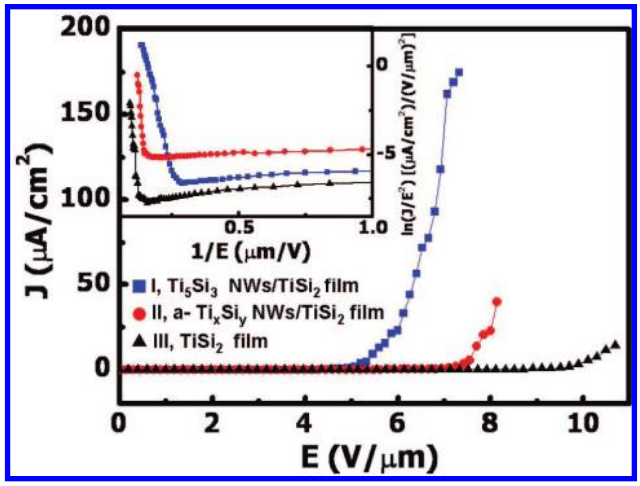

Figure 3. EFE current density as a function of applied electric field of samples **I**–**III**. The inset shows their corresponding F−N plots.

becomes extended.[25] All these reasons caused the Si concentration on the surface to decrease at this stage. As a consequence, the $TiSi_x$ clusters nucleated are Ti-rich. Because Ti_5Si_3 has the highest melting point and the lowest standard heat of formation among all of the titanium silicide phases, we suggest that Ti_5Si_3 should be the first silicide phase solidified.[26] Further migration and coalescence of small titanium silicide clusters to these nucleation sites elongates them into the observed Ti_5Si_3 NWs.

Electron field emission (EFE) properties and the corresponding Fowler−Nordheim (F−N) plots of the samples are illustrated in Figure 3.[27] Important EFE parameters extracted from the J−E curves, including the turn-on field E_0, which is defined as the electric field required to produce a current density of 10 μA cm^{-2}, and the field enhancement factor β, calculated from the equation $\beta = \phi^{3/2}/\phi_e$,[27] where ϕ is the work-function of the studied material and ϕ_e is the effective work-function derived from the slope of the F−N plot, are listed in Table 1. Among the samples studied, **I**, which is Ti_5Si_3 NWs on $TiSi_2$, shows a markedly superior EFE property compared to the others. The solid squares in Figure 3 illustrate that E_0 of **I** is only 5.4 V/μm. Sample **II**, which is composed of a-Ti_xSi_y NWs on $TiSi_2$, displays a higher E_0 of 7.6 V/μm while sample **III**, which is the C54-$TiSi_2$ thin film, shows the highest E_0 of 10.4 V/μm. We assume that the work functions ϕ of the $TiSi_2$ thin film and the Ti_5Si_3 NWs are the same as their bulk materials, that is, $\phi_{TiSi2} = 4.53$ eV and $\phi_{Ti5Si3} = 3.71$ eV.[15] Then, we can calculate β from ϕ and ϕ_e. ϕ_e values are proportional to the slopes of the F−N plots shown in Figure 3. For sample **I**, Ti_5Si_3 NWs/$TiSi_2$, we suppose that most electrons were emitted from the Ti_5Si_3 NWs because they were closer to the anode and were under higher electric field than the $TiSi_2$ film below. Thus, the β value of **I**, estimated using ϕ_{Ti5Si3} and the ϕ_e value of **I**, is 816. This result can be regarded as $\beta_{Ti5Si3NWs}$, the β value of Ti_5Si_3 NWs. It is higher than the reported β-value of $TiSi_2$ NWs, which is 500.[9a] The β-value of sample **III** is estimated to be 343. The value is high for a thin film. This may be the result from the surface roughness of **III**. Since there is no ϕ value available for a-Ti_xSi_y, it is not possible to estimate the β-value of **II**. Even though the SEM images demonstrated that **II** and **I** had similar entangled morphology, it appears that **II** could not perform better than **I** did. The amorphous NWs on **II** may not emit electrons as efficiently as the ones on **I**. By assuming that the ϕ value of a-Ti_xSi_y is close to those of various silicides, we can expect that the β-value of a-Ti_xSi_y NWs is between the values found for samples **I** and **III**.

In conclusion, this study is the first growth of Ti_5Si_3 NWs on C54-$TiSi_2$ thin films through a unique CVD process without additional catalyst. The diameters of the NWs are about 20–50 nm and the lengths are several micrometers. The Ti_5Si_3 NWs show excellent field emission properties, a low turn-on field E_0 of 5.4 V/μm, and a high field enhancement factor β of 816. These notable results suggest that Ti_5Si_3 NWs could serve as a promising candidate for future field emission devices.

Acknowledgment. We are grateful for the support from the National Science Council and the Ministry of Education of Taiwan, the Republic of China.

Supporting Information Available: Experimental section, Auger depth profile, SEM, TEM, ED, EDX, and XRD (PDF). This material is available free of charge via the Internet at http://pubs.acs.org.

CM800079C

(25) Southwell, R. P.; Seebauer, E. G. *J. Electrochem. Soc.* **1997**, *144*, 2122.
(26) Wang, M. H.; Chen, L. J. *J. Appl. Phys.* **1992**, *71*, 5918.
(27) Fowler, R. H.; Nordheim, L. W. *Proc. R. Soc. London, Ser. A* **1928**, *119*, 173.